

Vapor Phase Synthesis of Zirconia Fine Particles from Zirconium Tetra-*Tert*-Butoxide

Pavel Moravec^{1*}, Jiří Smolík¹, Helmi Keskinen², Jyrki M. Mäkelä²,
Valeri V. Levdansky³

¹ *Institute of Chemical Process Fundamentals, Academy of Sciences of the Czech Republic,
Rozvojová 135, 165 02 Prague 6, Czech Republic.*

² *Institute of Physics, Tampere University of Technology, Tampere, Finland.*

³ *A. V. Luikov Heat and Mass Transfer Institute, National Academy of Sciences of Belarus, 15. P.
Brovka Str., Minsk 220072, Belarus.*

Abstract

Zirconia fine particles were synthesized by thermal and hydrothermal decomposition of zirconium tetra-*tert*-butoxide in an externally heated tube flow reactor with two inlet section arrangements - long or short inlet nozzle. Particle production and characteristics were studied in dependence on reactor temperature, precursor concentration, and flow rates through the reactor and the nozzle. Particle production was investigated by scanning mobility particle sizer, morphology of particles by scanning/transmission electron microscopy, crystallinity by X-ray diffraction and selected area electron diffraction and composition of particles by energy dispersive spectroscopy. The particle production and morphology were affected most of all by the chemistry of precursor decomposition and the inlet section arrangement. The influence of remaining parameters was less significant. Particle formation mechanisms in the reactor volume and on the reactor and nozzle walls are also discussed.

Keywords: MOCVD; nanoparticle synthesis; tube flow reactor.

* Corresponding author. Tel.: +420-220-390-245, Fax: +420-220-920-661

E-mail address: moravec@icpf.cas.cz

INTRODUCTION

Ceramic powders are widely used. 'Fumed' nanosized silica has been produced by flame techniques already long time ago. Also, titania and alumina have been produced both on laboratory and industrial scale (Pratsinis, 1998). Several techniques such as combustion flames and tube flow reactors are widely used for generation of nanoceramics.

Zirconia (ZrO_2) shows resistance to high temperatures and corrosion, and therefore zirconia powders have become increasingly important in a number of high-tech applications and as raw material for new ceramics. Several techniques are available for producing zirconia nanopowders such as sol/gel method (Yang *et al.*, 1996), pyrolysis (Mazdiyasi *et al.*, 1965; Adachi *et al.*, 1989; Fotou *et al.*, 2000; Srdić *et al.*, 2000; Keskinen *et al.*, 2004), spray pyrolysis (Lenggoro *et al.*, 2000; Limaye and Helble, 2002; Nimmo *et al.*, 2002; Limaye and Helble, 2003), hydrolysis (Ocaña *et al.*, 1992; Keskinen *et al.*, 2004) and microwave plasma (Vollath and Sickafus, 1992). Depending on the method different production rates and particle size ranges can be covered. Also the possibility of doping the particles has been studied (Adachi *et al.*, 1989). Most often utilization of the method is linked with the type of precursor. Usually in spray pyrolysis, precursor salts such as $Zr(NO_3)_2$ (Lenggoro *et al.*, 2000; Nimmo *et al.*, 2002), dissolved in a sprayed liquid, are used with final particle size given predominantly by the precursor concentration. Recently, Limaye and Helble (2004) produced separate zirconia particles of sizes well below 100 nm using spray pyrolysis of zirconium(IV) dinitrate oxide hydrate in alcohol solvents. Gas phase pyrolysis uses thermal decomposition of vaporized precursors such as chlorides (Fotou *et al.*, 2000) or organometallic compounds (Adachi *et al.*, 1989; Srdić *et al.*, 2000; Keskinen *et al.*, 2004). Vaporized $ZrCl_2$ was also used in plasma induced decomposition (Vollath and Sickafus, 1992). Methods using vapor phase synthesis are usually known to have high potential in generating nanosized particles (Pratsinis, 1998). Another advantage is a relatively simple experimental arrangement and moderate temperatures (500-1000°C) necessary for precursor decomposition. We have previously used externally heated tube reactor for preparation of binary TiO_2/SiO_2 particles by simultaneous decomposition of titanium tetraisopropoxide (TTIP) and tetraethyl orthosilicate (TEOS) (Moravec *et al.*, 2002). To achieve formation of composite particles we used a long inlet section nozzle in approximately 2/5 of the reactor length for initial separation of flows with TEOS and TTIP. However, formation of titania particles in this arrangement was substantially different from that using an ordinary short nozzle (Moravec *et al.*, 2001). In a recent study (Keskinen *et al.*, 2004), we prepared zirconia fine particles by thermal and hydrothermal decomposition of zirconium tetra-*tert*-butoxide (ZTBO) in a tube reactor with the above mentioned long inlet section nozzle. It was found that the final particle size was controlled mainly by the precursor vapor concentration, whereas crystallinity of the product by the reactor temperature. Nevertheless, we also observed formation of substantial

amounts of large particles, which we attributed to the catalytic effect of the nozzle wall on ZTBO decomposition (Bradley, 1989). To complete the study, two nozzle lengths have been used to obtain additional information about the process of zirconia synthesis, using zirconium tetra-*tert*-butoxide vapor as a precursor. The study has been performed for different reactor temperatures, precursor concentrations, and flow rates of the reaction mixture through the reactor.

METHODS

Decomposition of ZTBO

In the following text we will use the term pyrolysis for thermal decomposition of ZTBO in an inert carrier gas and the term hydrolysis or hydrothermal decomposition for precursor decomposition at elevated temperature in a carrier gas saturated with water vapor. Detailed mechanism of thermal decomposition of ZTBO in glass vessels and inert atmosphere was described in the literature (Bradley, 1989). Overall reaction stoichiometry for both pyrolysis and hydrolysis of ZTBO can be written as follows:



From Eq. (1) it is clear that water vapor finally appears in the reaction mixture even in thermal decomposition of ZTBO. Thus the pyrolysis in this system is not exactly pure pyrolysis because water can enter the decomposition process and, under some conditions, accelerate the process and influence the mechanism of particle formation. However, in hydrothermal decomposition the water vapor is present in the reaction mixture from the beginning and practically in an infinite excess.

Experimental set-up

The experimental set-up used here is very similar to the one used in the previous study (Keskinen *et al.*, 2004). Particles were synthesized in an externally heated tube flow reactor of length 55 cm and i.d. 2.7 cm using two different nozzles at the inlet for introducing the reaction mixture: a long nozzle of length 25 cm and i.d. 2.0 cm and a short one 1.3 cm long and of i.d. 1.2 cm. The deoxygenated, dry and particle free nitrogen, used as a carrier gas, was saturated with ZTBO vapor in an externally heated saturator. The precursor concentration was controlled by the flow rate through the saturator, whose temperature was kept at 45°C. Partial pressure of the precursor vapor and subsequently c_{ZTBO} were calculated from the equation (Bradley and Swanwick, 1959):

$$\log P = \log 133.334 + 51.0296 - 5281.72/T - 13.9703 \log T. \quad (2)$$

Where $P(\text{Pa})$ is the partial vapor pressure and $T(\text{K})$ absolute temperature of the saturator. Saturated carrier gas was then mixed with another stream of nitrogen and fed axially into the center of the reactor through a nozzle surrounded by a coaxial stream of nitrogen. In hydrothermal experiments the mixing stream of nitrogen was saturated with water vapor at laboratory temperature. A mixture of gas and particles leaving the reactor was cooled in a diluter by mixing with a stream of nitrogen. Flow rates of individual gas streams were controlled by electronic mass flowmeters Tesla 306 KA/RA and the temperatures of saturator and reactor by electronic temperature controllers RLC T48. Samples of particles were collected on Sterlitech Ag filters or deposited onto carbon coated Cu grids by the point-to-plate electrostatic precipitator.

In the earlier study (Keskinen *et al.*, 2004), where the precursor was introduced inside the reactor using a long inlet nozzle (length 25 cm), the precursor reacted first in the nozzle tubing followed by further decomposition in the reactor. In this study we have used both long (LN) and short nozzle (SN). The arrangement with the short nozzle (Fig. 1A) should reduce the residence time and hence the reaction in the nozzle and increase the residence time and hence the reaction in the reactor. Now that the short nozzle has been utilized, we have to re-explore the most important parameters of the system. To investigate the influence of the residence time both in the nozzle and the reactor, we have studied, in addition to reactor temperature (T_R) and precursor concentration (c_{ZTBO}), also the effects of total flow in the reactor (Q_R) and the precursor feed via the central flow (Q_{CF}). All these parameters are assumed to affect the particle synthesis. Based on the earlier results (Moravec *et al.*, 2001; Keskinen *et al.*, 2004) we expect that increasing the reactor temperature the particle size will decrease and increasing the precursor concentration, the particle yield will increase. The wall reactions, on the other hand, are assumed to have an effect on the larger particle yield.

Particle analysis

The particle size distribution was monitored by scanning mobility particle sizer (SMPS, TSI model 3934C or 3936L). Particle morphology was studied by scanning/transmission electron microscopy (SEM/TEM) on JEOL 2000FX or JEOL 2010. Crystallinity of the samples was obtained by selected area electron diffraction (SAED) and by X-ray diffraction (XRD) on Philips X'Pert APD. Analyses of chemical composition were carried out by energy dispersive spectroscopy (EDS), Noran Vantage connected to TEM and Thermo-Noran D-6823 connected to SEM (Hitachi S-4700).

RESULTS AND DISCUSSION

Particle production

The particle production mechanism in a tube reactor with a long nozzle has been studied recently (Keskinen *et al.*, 2004). Various experimental parameters are known to influence particle characteristics. Firstly, the reaction chemistry, thermal and hydrothermal reaction kinetics affect the particle formation and the final morphology of the particles. In the case of hydrothermal reaction, the reaction rate is higher than that of thermal decomposition. From earlier study it was also concluded that thermal decomposition of ZTBO produces agglomerates, the growth of which in the reactor is first collision-limited and later limited by coalescence. Instead, in the case of hydrothermal decomposition, spherical, only slightly agglomerated particles were observed and particle growth was assumed to be limited by collision. The new inlet nozzle arrangement in the reactor (Fig. 1A) should influence particle formation mainly via the residence times in different reactor zones. It could also create some differences in the temperature profiles (Fig. 1B). In the nozzle, the temperature is assumed to be lower than in the reactor because the flow velocities are higher. Finally, c_{ZTBO} in the nozzle is also higher than in the reactor itself, because the total mass of precursor is diluted only by a part of carrier gas corresponding to Q_{CF} . All the aspects above are assumed to hold for the nanoparticles formed via aerosol route (nucleation) from the gas phase in the reactor atmosphere. But, it is also expected that some amount of larger particles is formed by heterogeneous reaction due to the catalytic effect on the reactor glass walls. In such a case, the reactor geometry (Fig. 1A) will affect particle formation by reactor and nozzle wall surface areas.

Thermal decomposition of ZTBO

In this section we present particle production by thermal decomposition of ZTBO at both the short and long inlet section nozzle in dependence on T_{R} (300–500°C), c_{ZTBO} (1.5×10^{-7} – 4.4×10^{-7} mol/l), Q_{R} (400–600 cm³/min), and Q_{CF} (60–80% of Q_{R}). A basic set of experimental conditions was selected as follows: T_{R} 500°C, c_{ZTBO} 4.4×10^{-7} mol/l, Q_{R} 600 cm³/min, and Q_{CF} 60% of Q_{R} . The influence of the above mentioned individual process parameters on particle production and particle characteristics was investigated by changing one of the parameters around its basic value keeping the other ones constant.

The results in the form of particle size distributions illustrating the influence of reactor temperature on particle production with both inlet section nozzles are shown in Fig. 2. With increasing T_{R} , the number concentration (N_{t}) and particle size (d_{p}) decrease in both inlet section arrangements. At 500°C higher concentration and bigger particles were obtained in short nozzle inlet section arrangement.

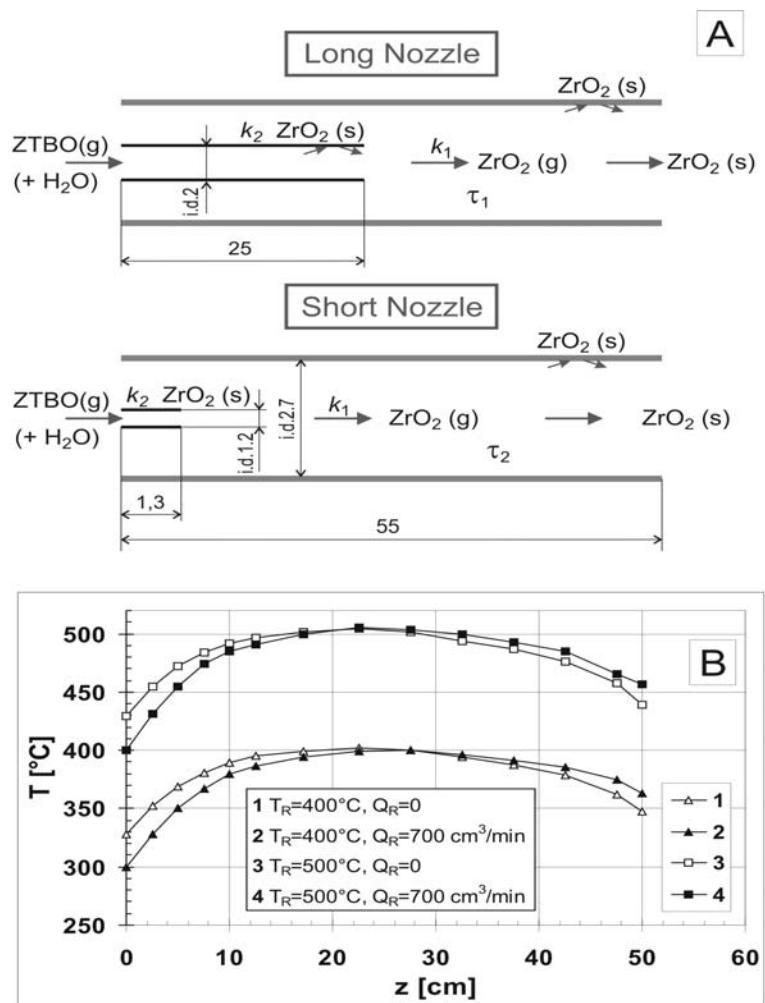


Fig. 1. A) Scheme of the ZTBO decomposition process in long and short nozzle inlet section arrangement: k_1 , k_2 kinetic constants of ZTBO decomposition by homogeneous and heterogeneous reaction, respectively, τ_1 , τ_2 residence times of reaction mixture in the reactor with long and short inlet nozzle, respectively, all dimensions are in cm; B) Axial temperature profiles in the reactor without inlet nozzle at various T_R and Q_R .

The influence of the other parameters was as follows: both number concentration and particle size increase with increasing c_{ZTBO} , number concentration increases also with Q_{CF} and shows maximum in dependence on Q_R . Mean particle size was generally larger at short nozzle arrangement.

Hydrothermal decomposition of ZTBO

Particle production by hydrolysis of ZTBO was generally rather different than that by pyrolysis under otherwise identical conditions. Particles had usually bimodal size distribution with the dominating small particle mode and with the small particle mode being almost an order of

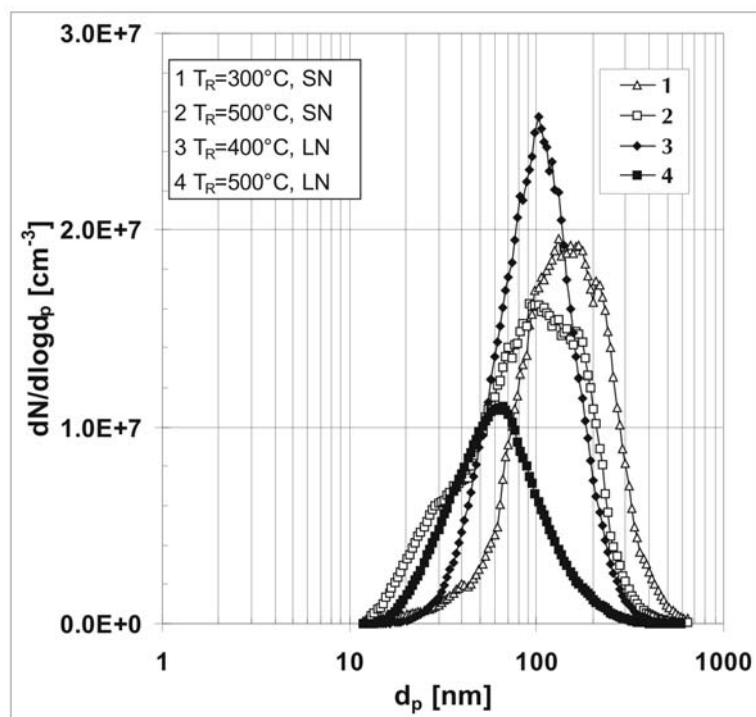


Fig. 2. Influence of T_R on particle size distributions generated by thermal decomposition of ZTBO at $c_{ZTBO} = 4.4 \times 10^{-7}$ mol/l, $Q_R = 600$ cm³/min, $Q_{CF} = 60\%$.

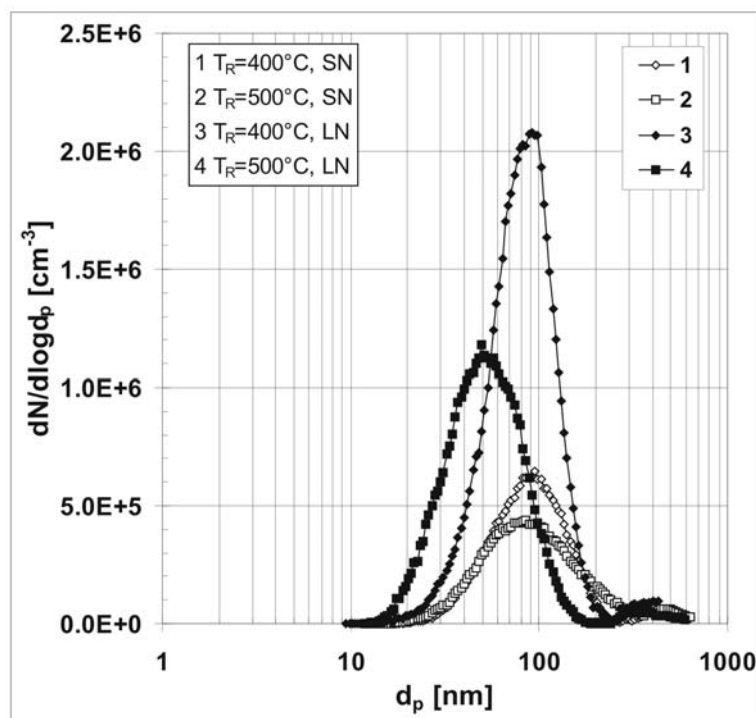


Fig. 3. Influence of T_R on particle size distributions generated by hydrothermal decomposition of ZTBO at $c_{ZTBO} = 4.4 \times 10^{-7}$ mol/l, $Q_R = 600$ cm³/min, $Q_{CF} = 60\%$.

magnitude lower than in the case of pyrolysis. A part of the large particle mode was typically at least partly out of the measuring range of SMPS.

On the other hand, the influence of process parameters on particle production showed rather similar trends as in the case of pyrolysis. As a comparison with thermal decomposition (Fig. 2) the influence of T_R on particle production is shown in Fig. 3.

Particle characteristics

Similarly as particle production, also particle characteristics were studied with special attention to four main combinations of experimental conditions; thermal and hydrothermal decompositions of ZTBO in both short and long inlet section arrangement.

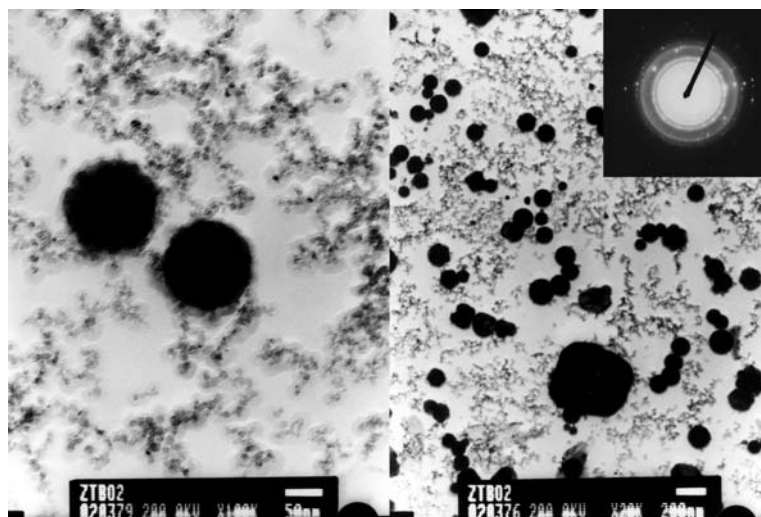


Fig. 4. Bright field TEM images and SAED pattern of a sample of particles prepared by pyrolysis at $T_R = 500^\circ\text{C}$, $c_{\text{ZTBO}} = 4.4 \times 10^{-7} \text{ mol/l}$, $Q_R = 600 \text{ cm}^3/\text{min}$, $Q_{\text{CF}} = 60\%$, with long nozzle at reactor inlet.

Morphology

The morphology of the produced particles varied remarkably. It was affected mainly by the chemistry of precursor decomposition and precursor concentration. The effect of remaining parameters was less pronounced. Particles prepared by pyrolysis with long nozzle at the reactor inlet are shown in Fig. 4. Most of them were spherical nanosized particles from 10-40 nm. But the amount of submicron-sized particles of various shapes from spherical particles with smooth surface, spherical or nearly spherical with rough surface to quite irregularly shaped particles could not be neglected. The irregularities were probably caused by incomplete coalescence of smaller particles (glued and deflated particles) on one hand and by formation of the crystalline phase on the other (angular particles). The degree of irregularity increased with the particle size. Comparing primary particle sizes from TEM pictures with particle size distributions obtained by

SMPS (curve 4 in Fig. 2), one can see that the primary particle size on TEM pictures is several times smaller than the mean particle size from SMPS distributions. This indicates that SMPS scanned already aggregates of primary particles.

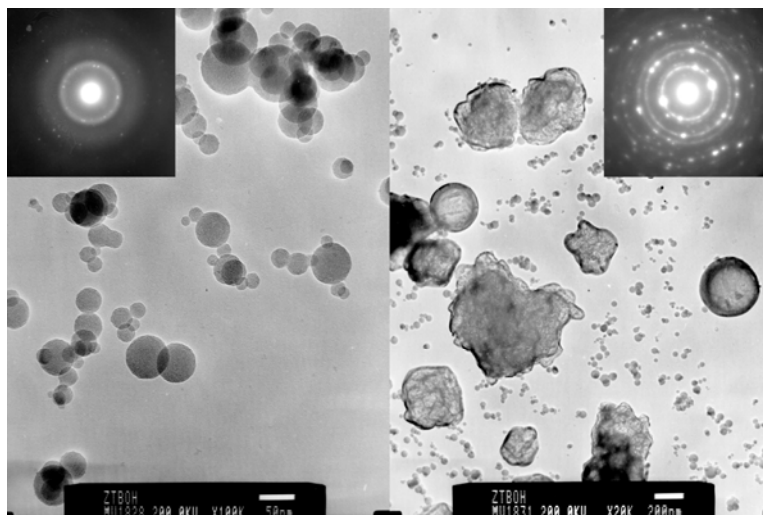


Fig. 5. Bright field TEM images and SAED patterns of a sample of particles prepared by hydrolysis at $T_R = 500^\circ\text{C}$, $c_{ZTBO} = 4.4 \times 10^{-7} \text{ mol/l}$, $Q_R = 600 \text{ cm}^3/\text{min}$, $Q_{CF} = 60\%$, with long nozzle at reactor inlet.

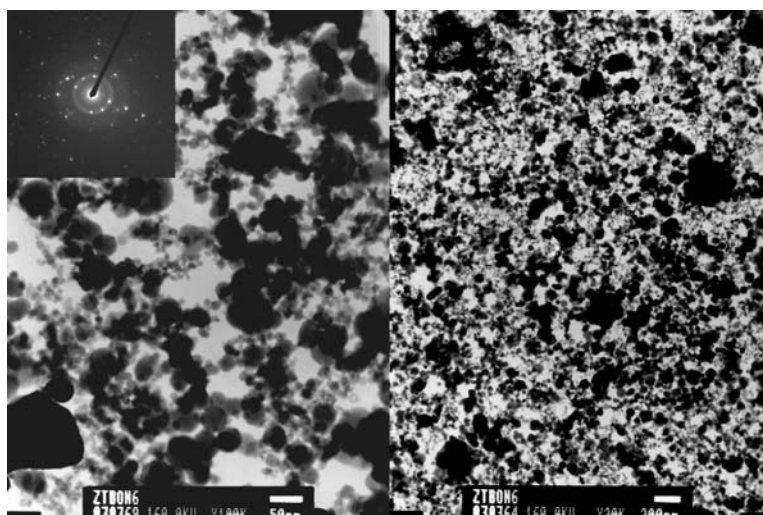


Fig. 6. Bright field TEM images and SAED pattern of a sample of particles prepared by pyrolysis at $T_R = 500^\circ\text{C}$, $c_{ZTBO} = 4.4 \times 10^{-7} \text{ mol/l}$, $Q_R = 600 \text{ cm}^3/\text{min}$, $Q_{CF} = 70\%$, with short nozzle at reactor inlet.

The morphology of particles prepared by hydrolysis with long nozzle at the reactor inlet is shown in Fig. 5. While large particles had very similar morphology to those prepared by pyrolysis, small particles were different. They were much larger than small pyrolytic particles,

typically above 50 nm, spherical, less agglomerated and their size was in good agreement with the results obtained by SMPS (curve 4 in Fig. 3). This fact demonstrates that SMPS detected individual particles in hydrothermal decomposition.

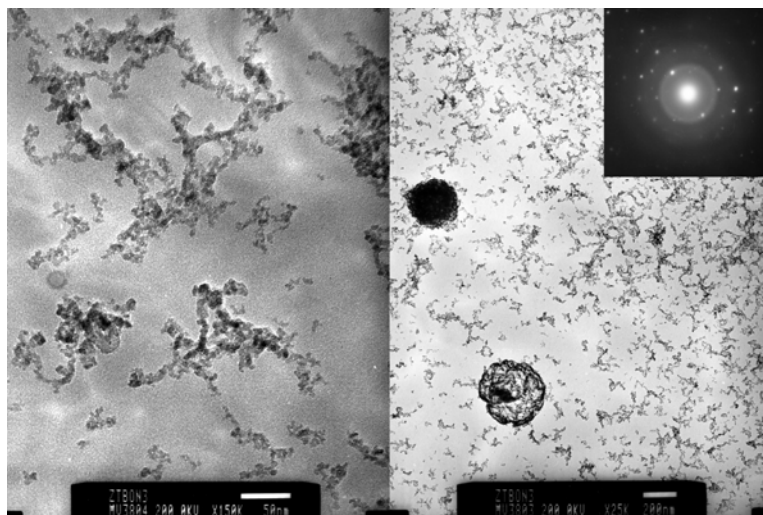


Fig. 7. Bright field TEM images and SAED pattern of a sample of particles prepared by pyrolysis at $T_R = 400^\circ\text{C}$, $c_{\text{ZTBO}} = 1.5 \times 10^{-7}$ mol/l, $Q_R = 600$ cm³/min, $Q_{\text{CF}} = 60\%$, with short nozzle at reactor inlet.

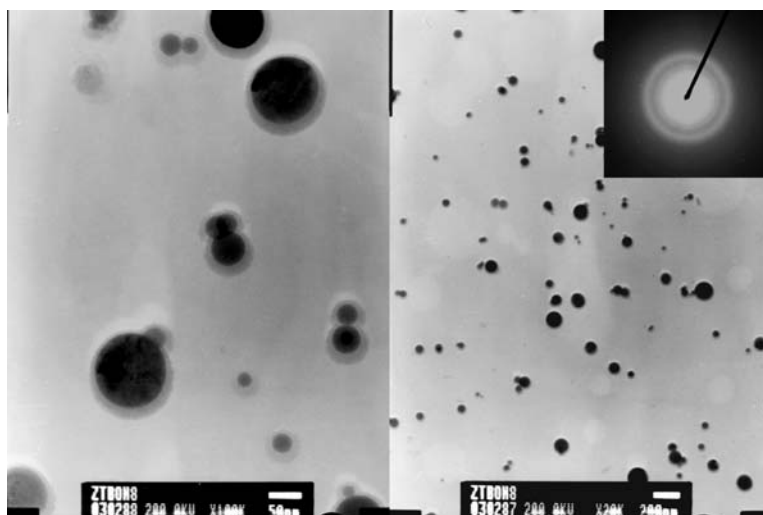


Fig. 8. Bright field TEM images and SAED pattern of a sample of particles prepared by hydrolysis at $T_R = 500^\circ\text{C}$, $c_{\text{ZTBO}} = 4.4 \times 10^{-7}$ mol/l, $Q_R = 600$ cm³/min, $Q_{\text{CF}} = 60\%$, with short nozzle at reactor inlet.

Replacing long nozzle at the reactor inlet by short one resulted in a substantial modification of large particle morphology. A sample of particles prepared by pyrolysis can be seen in Fig. 6. The amount of irregular-shaped submicron sized particles substantially decreased, and in addition to

spherical nanoparticles below 50 nm, there was also present an abundant fraction of medium-sized spherical particles between 50 and 100 nm. At a very low precursor concentration, this medium-sized fraction did not appear and aggregates of very small particles (10 - 20 nm) with only few submicron-sized particles were produced (see Fig. 7). The morphology of particles produced by hydrolysis (see Fig. 8) was rather similar to that in long nozzle arrangement (Fig. 5). Small particles were again spherical but larger than in long nozzle arrangement and the amount of submicron-sized particles seemed to be lower.

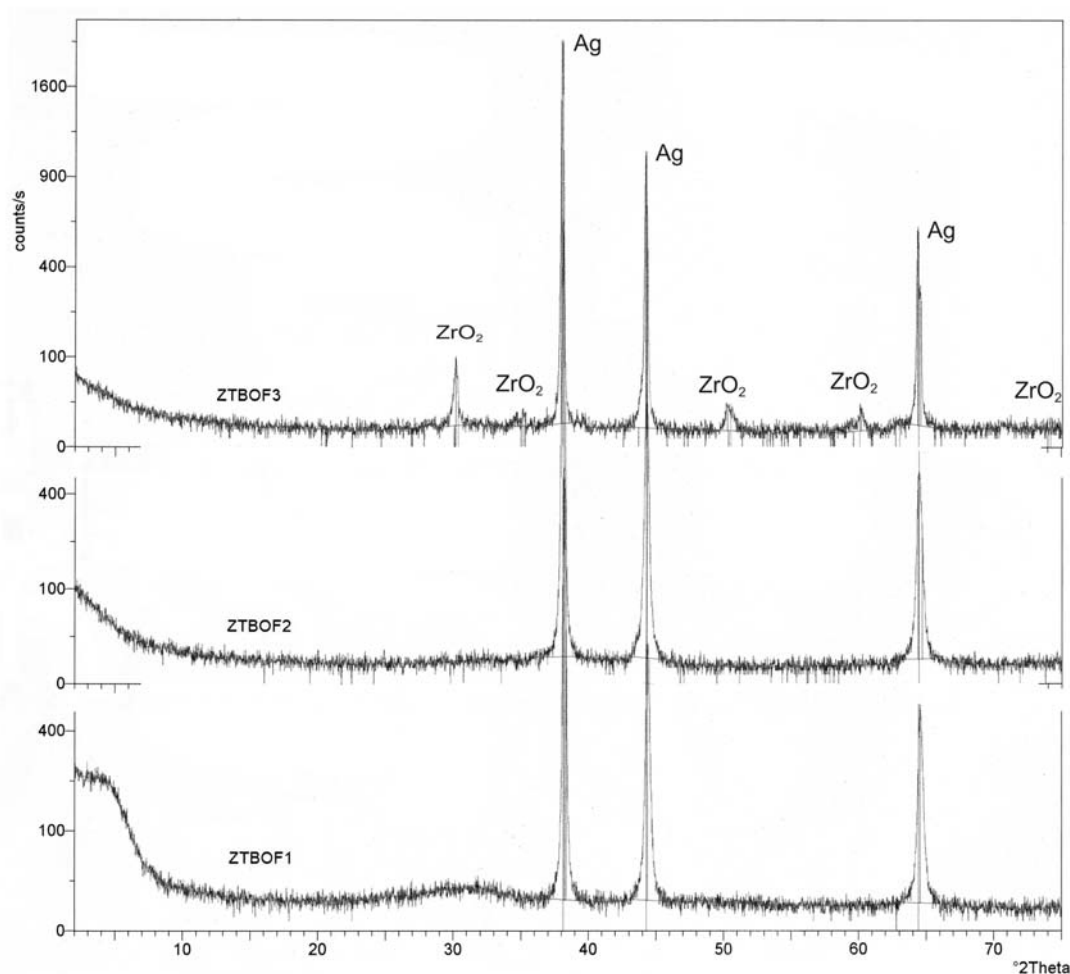


Fig. 9. XRD patterns of samples of particles prepared by pyrolysis in short inlet nozzle arrangement and T_R 300°C (ZTBOF1), 400°C (ZTBOF2), and 500°C (ZTBOF3). Ag denotes Silver 3C (ref. pattern 04-0783), ZrO₂–FCC ZrO₂ (07-0337).

Crystallinity and composition

The crystallinity and crystalline structure of the prepared particles were investigated by XRD and by SAED. While XRD showed visible peaks of ZrO₂ only in the particles prepared at 500°C

(see Fig. 9), dark-field TEM images and SAED confirmed the presence of some portion of the crystalline phase also in the particles prepared at 400 and even at 300°C. Electron diffraction patterns of all tests but one showed face-centred cubic (FCC) ZrO₂ in the samples. In one test of the sample prepared at T_R 400°C by thermal decomposition using long inlet nozzle, the FCC ZrO₂ diffraction pattern was detected in submicron-sized particle (Keskinen *et al.* 2004). Based on SAED patterns (see Fig. 4–Fig. 8) and dark-field images of the samples, we can conclude that the particles prepared by pyrolysis are more crystalline than those obtained by hydrolysis and that the proportion of crystalline phase increases with increasing particle size and T_R .

The results of SAED were confirmed by EDS analyses of chemical composition. The zirconium to oxygen ratio close to 0.5 was detected by EDS in the particles that showed FCC ZrO₂ electron diffraction pattern, while in the particle detected as FCC ZrO, the value of the Zr-to-O ratio was approaching to 1.

Discussions of the particle formation process

From preceding paragraphs it seems probable that particle formation is a complex process consisting of several substeps. First, it is chemical reaction in the reactor volume, which depends on temperature, precursor concentration and chemistry of precursor decomposition (concentration of water vapor). From axial temperature profiles in the reactor (see Fig. 1B), we can expect steep variation of the rate of chemical reaction inside the reactor. As the next step, formation of primary particles by nucleation and Brownian coagulation occurs. Further growth of particles continues by condensation of the rest of the product vapors and by coagulation of primary particles. Coagulation of primary particles seems to be coalescence-limited mostly in the case of pyrolysis, and collision-limited in the case of hydrolysis.

Simultaneously with the particle formation via homogeneous reaction in the gas phase, also heterogeneous decomposition of precursor occurs in the vicinity of the reactor and nozzle walls. This reaction is catalyzed by the glass surface (Bradley, 1989) and, therefore, additional formation of particles takes place. It can be expected that in this process the rate-limiting steps are transport phenomena to and from the surface. Hence, the particle formation by this mechanism is dependent on reactor temperature and precursor concentration and, on the other hand, rather independent of the presence of water vapor in the reaction mixture due to water formed by dehydration reaction in the reaction region. As a result, formation of a deposit and subsequent re-entrainment and eventual coagulation can cause formation of large, irregularly shaped particles. The main parameter affecting the surface reaction is the surface of the inner nozzle wall because contact of precursor with the reactor wall is hampered by sheath flow of carrier gas. In the case of short nozzle this surface is rather small: however, the probability that precursor vapors break up the sheath flow and reach the reactor wall is higher. With increasing

flow rate through the nozzle, the consumption of precursor by surface reaction decreases and the concentration of small particles increases.

A shorter residence time in the hot zone of the reactor in the long nozzle arrangement results in coalescence limited agglomeration of primary particles in thermal decomposition of ZTBO (Fig. 4). Interestingly, in short nozzle arrangement under otherwise identical conditions, also spherical non-agglomerated middle-size particles (~50 nm) were formed (see Fig. 6). Formation of this particle fraction can be the result of accompanying hydrolysis induced by water produced by thermal decomposition of ZTBO in some reactor zones. However, at lower precursor concentrations (or lower T_R), formation of primary particles is slower, their residence time in the hot zone is shorter and, as a result, incompletely coagulated particles are produced (see Fig. 7). On the other hand, in hydrothermal decomposition of ZTBO (see Fig. 5), the small-mode particles were always spherical and almost non-agglomerated, so that we can expect much faster chemical reaction in the reactor volume and complete coalescence of primary particles.

According to the results obtained under different conditions and nozzle configurations, the precursor concentration seems to systematically increase the particle size produced via homogeneous reaction but not necessarily the particle size via heterogeneous wall reaction. Also, the short nozzle configuration having a longer residence time tends to give larger particle size than the long nozzle configuration. This applies to both pyrolysis (Fig. 4 and Fig. 6) and hydrolysis (Fig. 5 and Fig. 8) of ZTBO.

CONCLUSIONS

Fine zirconia particles were produced by pyrolysis and hydrolysis of ZTBO in an externally heated tube reactor with a long or short nozzle at the reactor inlet. Generally, the produced particles consisted of two size modes. The small particle mode contained aggregates of spherical nanoparticles of the size well below 50 nm (pyrolysis) or spherical particles of the size between 50 and 100 nm (hydrolysis). The large particle mode consisted of irregularly shaped submicron-sized particles (both pyrolysis and hydrolysis). The amount of submicron sized particles was substantially reduced using inlet section arrangement with a short nozzle.

The particle production and morphology were remarkably affected by the choice of pyrolysis or hydrolysis but also, to some extent, by nozzle arrangement and the reactor temperature, precursor concentration and flow rates used. The length of the nozzle determined the residence time both in the nozzle and in the reactor. Here, a longer residence time in the reactor (i.e. short nozzle) resulted in larger particles via homogeneous reaction. On the other hand, a longer residence time in the nozzle (i.e. long nozzle) resulted in more particles via heterogeneous reaction. The reactor temperature increased the crystallinity (FCC ZrO_2) of particles. SAED analysis already indicated some amount of crystalline structure at 300°C. The precursor

concentration increased the particle size. Finally, the particle concentration could be increased by increasing the central flow both in pyrolysis and hydrolysis.

ACKNOWLEDGMENTS

This work was supported by Grant Agency of the Czech Republic (grants No. 104/02/1079 and 104/07/1093), the Finnish Academy of Science and Letters (project No. 201808) and the Academy of Sciences of the Czech Republic (project No. K4050111). EDS analyses were performed by Doc. Minnamari Vippola, Institute of Materials Science, Tampere University of Technology, TEM and SAED analyses were performed by Doc. Minnamari Vippola and Doc. Bohumil Smola, Faculty of Mathematics and Physics, Charles University. XRD analyses were performed by Mr. Dobrovolný, Geological Institute, Academy of Sciences of the Czech Republic.

REFERENCES

- Adachi, M., Okuyama, K., Moon, S., Tohge, N. and Kousaka, Y. (1989). Preparation of Ultrafine Zirconium Dioxide Particles by Thermal Decomposition of Zirconium Alkoxide Vapour. *J. Mater. Sci.* 24: 2275-2280.
- Bradley, D.C. (1989). Metal Alkoxides as Precursors for Electronic and Ceramic Materials. *Chem. Rev.* 89: 1317-1322.
- Bradley, D.C. and Swanwick, D.J. (1959). Vapour Pressures of Metal Alkoxides. 2. Zirconium Tetra-Tert-Butoxide and Tetra-Tert-Amyloxyde. *J. Chem. Soc.* 748-752.
- Fotou, G.P., Kodas, T.T. and Anderson, B. (2000). Coating Titania Aerosol Particles with ZrO₂, Al₂O₃/ZrO₂, and SiO₂/ZrO₂ in a Gas-Phase Process. *Aerosol Sci. Technol.* 33: 557-571.
- Keskinen, H., Moravec, P., Smolík, J., Levdansky, V.V., Mäkelä, J.M. and Keskinen, J. (2004). Preparation of ZrO₂ Fine Particles by CVD Process: Thermal Decomposition of Zirconium Tert-Butoxide Vapor. *J. Mater. Sci.* 39: 4923-4929.
- Lenggoro, I.W., Hata, T., Iskandar, F., Lunden, M.M. and Okuyama, K. (2000). An Experimental and Modeling Investigation of Particle Production by Spray Pyrolysis Using a Laminar Flow Aerosol Reactor. *J. Mater. Res.* 15: 733-743.
- Limaye, A.U. and Helble, J.J. (2002). Morphological Control of Zirconia Nanoparticles through Combustion Aerosol Synthesis. *J. Am. Ceram. Soc.* 85: 1127-1132.
- Limaye, A.U. and Helble, J.J. (2003). Effect of Precursor and Solvent on Morphology of Zirconia Nanoparticles Produced by Combustion Aerosol Synthesis. *J. Am. Ceram. Soc.* 86: 273-278.
- Limaye, A.U. and Helble, J.J. (2004). Secondary Atomization as a Mechanism for Controlling the Size of Ceramic Nanoparticles Produced by Combustion Aerosol Synthesis. *J. Aerosol Sci.* 35: 599-610.

- Mazdiyasi, K.S., Lynch, C.T. and Smith, J.S. (1965). Preparation of Ultra-High-Purity Submicron Refractory Oxides. *J. Am. Ceram. Soc.* 48: 372-375.
- Moravec, P., Smolík, J. and Levdansky, V.V. in: Korhonen, H. (Ed.) Czech-Finnish Aerosol Symposium, Prague (Czech Republic), 23-26 May 2002; *Report Ser. Aerosol Sci.* No. 56, pp. 119-122.
- Moravec, P., Smolík, J. and Levdansky, V.V. (2001). Preparation of TiO₂ Fine Particles by Thermal Decomposition of Titanium Tetraisopropoxide Vapor. *J. Mater. Sci. Lett.* 20: 2033-2037.
- Nimmo, W., Hind, D., Ali, N.J., Hampartsoumian E. and Milne, S.J. (2002). The Production of Ultrafine Zirconium Oxide Powders by Spray Pyrolysis. *J. Mater. Sci.* 37: 3381-3387.
- Ocaña, M., Fornés, V. and Serna, C.J. (1992). A Simple Procedure for the Preparation of Spherical Oxide Particles by Hydrolysis of Aerosols. *Ceram. Int.* 18: 99-106.
- Pratsinis, S.E. (1998). Flame Aerosol Synthesis of Ceramic Powders. *Prog. Energy Combust. Sci.* 24: 197-219.
- Srdić, V.V., Winterer, M. and Hahn, H. (2000). Sintering Behavior of Nanocrystalline Zirconia Prepared by Chemical Vapor Synthesis. *J. Am. Ceram. Soc.* 83: 729-736.
- Vollath, D. and Sickafus, K.E. (1992). Synthesis of Nanosized Ceramic Oxide Powders by Microwave Plasma Reactions. *Nanostruct. Mater.* 1: 427-437.
- Yang, C., Hong, B. and Chen, J. (1996). Production of Ultrafine ZrO₂ and Y-Doped ZrO₂ Powders by Solvent Extraction from Solutions of Perchloric and Nitric Acid with Tri-n-Butyl Phosphate in Kerosene. *Powder Technol.* 89: 149-155.

Received for review, March 8, 2007

Accepted, August 8, 2007